Author Manuscript

Author Manuscript

Author Manuscript

Author Manuscript

HHS Public Access

Author manuscript

Cell Rep. Author manuscript; available in PMC 2017 December 06.

Published in final edited form as:

Cell Rep. 2016 December 06; 17(10): 2596–2606. doi:10.1016/j.celrep.2016.11.010.

Low CD38 Identifies Progenitor-like Inflammation-Associated Luminal Cells that Can Initiate Human Prostate Cancer and Predict Poor Outcome

Xian Liu[1], **Tristan R. Grogan**[3], **Haley Hieronymus**[4], **Takao Hashimoto**[1], **Jack Mottahedeh**[1], **Donghui Cheng**[5], **Lijun Zhang**[2], **Kevin Huang**[2], **Tanya Stoyanova**[6,15], **Jung Wook Park**[6], **Ruzanna O. Shkhyan**[1], **Behdokht Nowroozizadeh**[7], **Matthew B. Rettig**[8,9,10,11], **Charles L. Sawyers**[4], **David Elashoff**[3,11], **Steve Horvath**[12,13], **Jiaoti Huang**[5,7,11,16], **Owen N. Witte**[2,5,6,11,14], and **Andrew S. Goldstein**[1,5,10,11,17,*]

[1]Molecular, Cell and Developmental Biology, University of California, Los Angeles, Los Angeles, CA 90095, USA

[2]Molecular and Medical Pharmacology, David Geffen School of Medicine, University of California, Los Angeles, Los Angeles, CA 90095, USA

[3]Department of Medicine Statistics Core, David Geffen School of Medicine, University of California, Los Angeles, Los Angeles, CA 90095, USA

[4]Programs in Human Oncology and Pathogenesis, Memorial Sloan Kettering Cancer Center, New York, NY 10065, USA

[5]Eli and Edythe Broad Center of Regenerative Medicine and Stem Cell Research, University of California, Los Angeles, Los Angeles, CA 90095, USA

[6]Microbiology, Immunology and Molecular Genetics, University of California, Los Angeles, Los Angeles, CA 90095, USA

[7]Pathology and Laboratory Medicine, David Geffen School of Medicine, University of California, Los Angeles, Los Angeles, CA 90095, USA

[8]Division of Hematology-Oncology, David Geffen School of Medicine, University of California, Los Angeles, Los Angeles, CA 90095, USA

This is an open access article under the CC BY-NC-ND license (http://creativecommons.org/licenses/by-nc-nd/4.0/).

[*]Correspondence: agoldstein@mednet.ucla.edu.

[15]Present address: Department of Radiology, Canary Center at Stanford for Cancer Early Detection, Stanford University School of Medicine, Palo Alto, CA 94304, USA

[16]Present address: Department of Pathology, Duke University School of Medicine, Durham, NC 27710, USA

[17]Lead Contact

ACCESSION NUMBERS

The accession number for the data reported in this paper is GEO: GSE89050.

SUPPLEMENTAL INFORMATION

Supplemental Information includes Supplemental Experimental Procedures, seven figures, and six tables and can be found with this article online at http://dx.doi.org/10.1016/j.celrep.2016.11.010.

AUTHOR CONTRIBUTIONS

X.L. and A.S.G. performed the majority of experiments and wrote and edited the manuscript. T.H., J.M., D.C., L.Z., K.H., T.S., and R.O.S. performed experiments. T.R.G., D.E., S.H., H.H., and C.L.S. performed statistical analysis. J.W.P. developed organoid transformation methods. B.N. and J.H. provided pathology expertise. M.B.R. provided tissue microarrays. J.H. and O.N.W. edited and contributed to writing of the manuscript.

Author Manuscript Author Manuscript Author Manuscript Author Manuscript

[9]VA Greater Los Angeles Healthcare System, Los Angeles, CA 90024, USA

[10]Urology, David Geffen School of Medicine, University of California, Los Angeles, Los Angeles, CA 90095, USA

[11]Jonsson Comprehensive Cancer Center, University of California, Los Angeles, Los Angeles, CA 90095, USA

[12]Human Genetics, David Geffen School of Medicine, University of California, Los Angeles, Los Angeles, CA 90095, USA

[13]Biostatistics, UCLA Fielding School of Public Health, University of California, Los Angeles, Los Angeles, CA 90095, USA

[14]Howard Hughes Medical Institute, University of California, Los Angeles, Los Angeles, CA 90095, USA

SUMMARY

Inflammation is a risk factor for prostate cancer, but the mechanisms by which inflammation increases that risk are poorly understood. Here, we demonstrate that low expression of CD38 identifies a progenitor-like subset of luminal cells in the human prostate. CD38^{lo} luminal cells are enriched in glands adjacent to inflammatory cells and exhibit epithelial nuclear factor κB (NF-κB) signaling. In response to oncogenic transformation, CD38^{lo} luminal cells can initiate human prostate cancer in an in vivo tissue-regeneration assay. Finally, the CD38^{lo} luminal phenotype and gene signature are associated with disease progression and poor outcome in prostate cancer. Our results suggest that prostate inflammation expands the pool of progenitor-like target cells susceptible to tumorigenesis.

In Brief

Chronic inflammation of the prostate is a risk factor for cancer, but how inflammation increases disease risk remains poorly defined. Liu et al. show that luminal progenitor cells expressing low levels of CD38 are expanded around inflammation, and these progenitors are target cells that can initiate human prostate cancer.

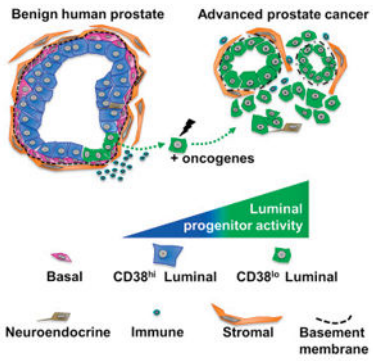

Author Manuscript Author Manuscript Author Manuscript Author Manuscript

INTRODUCTION

An inflammatory microenvironment is a critical component driving tumorigenesis, from cancer initiation to metastasis to end-stage treatment-resistant lethal disease (Das Roy et al., 2009; Gurel et al., 2014; Liu et al., 2013; Wang et al., 2015). In many adult tissues, cancers originate in sites of chronic inflammation (Coussens and Werb, 2002). It is hypothesized that sustained proliferative signals from inflammatory cells can cooperate with oncogenic events to promote tumorigenesis (De Marzo et al., 2007). Mouse models have been developed that recapitulate features of inflammation in the tumor microenvironment and demonstrate a role for defined immune cell types and inflammatory cytokines in cancer initiation and progression (Ammirante et al., 2010; Garcia et al., 2014). Few studies have investigated the functional consequences of inflammation in human epithelial tissues.

Chronic inflammation of the prostate is a risk factor for aggressive prostate cancer (Gurel et al., 2014; Sfanos and De Marzo, 2012; Shafique et al., 2012), as men with chronic inflammation in benign tissues have greater than double the risk for developing high-grade disease compared to men with no inflammation in their benign biopsy cores (Gurel et al., 2014). Groundbreaking work from De Marzo and colleagues has defined a series of histological changes associated with chronic inflammation in the human prostate known as proliferative inflammatory atrophy (PIA) as a likely precursor for prostate cancer (De Marzo et al., 1999, 2007). In PIA, the luminal epithelial layer in close proximity to infiltrating immune cells is described as having an atrophic appearance with an increased proliferative index, suggesting a regenerative response (De Marzo et al., 2003). Luminal cells associated with PIA exhibit reduced androgen signaling and increased expression of the anti-apoptotic factor BCL2 (De Marzo et al., 1999, 2003). PIA cells are thought to exhibit an intermediate state of differentiation between basal and luminal cells and are predicted to serve as target cells in prostate tumorigenesis (van Leenders et al., 2003). Several groups have modeled inflammation in the mouse prostate using a variety of approaches, including bacterial infection (Elkahwaji et al., 2009; Khalili et al., 2010; Kwon et al., 2014), high-fat diet (Kwon et al., 2016), and adoptive transfer of prostate-targeting T cells (Haverkamp et al., 2011), demonstrating that prostatic inflammation is associated with increased epithelial proliferation. However, mouse models may not recapitulate the complex environment of aged human prostate tissues exposed to chronic inflammation for years prior to the development of prostate cancer (Gurel et al., 2014).

Lineage tracing in the mouse has demonstrated that both basal and luminal cells are sufficient to initiate prostate cancer following *Pten* deletion, with differences in tumor outcome depending on the genetic background and status of *Nkx3-1* (Choi et al., 2012; Lu et al., 2013; Wang et al., 2013). Luminal cells can initiate murine prostate cancer in diverse genetically engineered mouse models (Wang et al., 2014), while purified basal cells can respond to a range of oncogene combinations to generate murine tumors using a tissue-regeneration approach (Lawson et al., 2010). In the human prostate, we and others have demonstrated that basal cells isolated from benign human prostate can give rise to tumors following oncogenic transformation (Goldstein et al., 2010; Stoyanova et al., 2013; Taylor et al., 2012). To date, luminal cells in the human prostate have only been shown to initiate indolent-like tumors with limited proliferation (Park et al., 2016), perhaps due to the low rate

Author Manuscript Author Manuscript Author Manuscript Author Manuscript

of proliferation among luminal cells (De Marzo et al., 1999). In contrast, luminal cell proliferation is increased in regions associated with inflammation in human prostate (De Marzo et al., 1999), suggesting that luminal cells isolated from regions with inflammation may exhibit progenitor cell features and give rise to aggressive prostate cancer.

Here, we report that expression of the luminal cell marker CD38 is heterogeneous in the human prostate. We used low expression of CD38 to isolate a subset of p63-negative, keratin 14 (K14)-negative, keratin 18 (K18)-positive luminal cells from primary benign human prostate with unique functional and molecular properties compared to $CD38^{hi}$ luminal cells. Human prostate $CD38^{lo}$ $CD38^{lo}$ luminal cells are expanded in regions with inflammation, express markers of PIA, and are enriched for progenitor activity. In human tissues, CD38 is inversely correlated with prostate cancer progression and low CD38 mRNA in tumors is prognostic for biochemical recurrence and metastasis. Finally, $CD38^{lo}$ luminal cells can initiate prostate cancer in response to oncogenic transformation using a human tissue regeneration model in immune-deficient mice. These collective results support inflammation-associated luminal cells as a target cell for aggressive prostate cancer.

RESULTS

Differential Expression of CD38 Enables Isolation of Two Distinct Luminal Subsets

CD38 is reported as a marker of luminal cells in the human prostate (Kramer et al., 1995), and gene expression studies demonstrate that CD38 mRNA can distinguish basal from luminal cells (Smith et al., 2015). We measured cell-surface expression of CD38 by flow cytometry and confirmed that within the $EpCAM^{+}$ $CD45^{-}$ epithelial fraction, CD38 is expressed by $CD26^{+}$ luminal cells, but not by CD49f-hi basal cells (Figure 1A). Upon performing immunohistochemical staining for CD38 in human prostate tissue, we noted heterogeneous staining within the luminal layer, including areas where CD38 expression was reduced within individual glands (Figure 1B).

We set out to viably isolate luminal cells based on variations in surface expression of CD38 using fluorescence-activated cell sorting (FACS). After removing $CD45^{+}$ immune cells and gating on $EpCAM^{+}$ epithelial cells, we observed three cell populations based on expression of CD49f and CD38 (Figure 1C) in preparations of dissociated cells isolated from benign human prostate tissue. Intracellular flow cytometry revealed that both CD49f-lo $CD38^{hi}$ and $CD49f^{lo}$ $CD38^{lo}$ subsets expressed high levels of the luminal marker K18 (Figures 1D and S1A). Western blot analysis demonstrated that basal markers p63 and K14 are not expressed in either luminal subset (Figure 1E). We noted elevated expression of keratin 5 (K5), a marker of a proposed intermediate-type luminal cell (van Leenders et al., 2003), in $CD38^{lo}$ compared to $CD38^{hi}$ luminal cells (Figure S1B). Following cell isolation, cell diameters were measured to examine differences in size among the three epithelial populations. $CD38^{lo}$ luminal cells demonstrated an average diameter intermediate between basal and $CD38^{hi}$ luminal cells (Figure 1F). These findings indicate that CD38 stratifies luminal cells into two distinct subpopulations. Importantly, $CD38^{lo}$ luminal cells do not express CD26 by flow cytometry (Figure S1C). These data indicate that $CD38^{lo}$ luminal cells are distinct from $CD26^{+}$ luminal cells and represent a population not previously investigated in prior studies (Karthaus et al., 2014; Park et al., 2016; Stoyanova et al., 2013).

Author Manuscript Author Manuscript Author Manuscript Author Manuscript

CD38^{lo} Luminal Cells Are Enriched for Progenitor Activity Compared to CD38^{hi} Luminal Cells

In order to test the functional capacity of distinct luminal subsets, it is important to remove any potential contaminating basal cells that are highly clonogenic in progenitor assays (Goldstein et al., 2008; Karthaus et al., 2014; Park et al., 2016). We used a double-sorting approach to isolate highly purified preparations of CD38^{lo} and CD38^{hi} luminal cells from benign human prostate tissue and confirmed an absence of basal cells based on lack of expression of CD49f (Figure 2A) and p63 (Figures S2A and S2B). In a two-dimensional colony-forming assay and a three-dimensional sphere-forming assay (Lawson et al., 2010; Lukacs et al., 2010), CD38^{lo} luminal cells exhibited progenitor activity intermediate between the highly clonogenic basal cells and the CD38^{hi} luminal cells (Figures 2B and 2C). In a culture system adapted for the growth of human prostate-like tissue in vitro (Karthaus et al., 2014), CD38^{lo} luminal cells were highly (4- to 5-fold) enriched for organoid formation compared to CD38^{hi} luminal cells (Figure 2D). CD38^{lo} luminal cell-derived organoids contained cells expressing both basal (K5 and p63) and luminal (K8) markers (Figures 2E and S2C), similar to what has been reported for CD26^{+} luminal cells (Karthaus et al., 2014). When double-sorted cells were plated at single-cell density and visually confirmed, 5% (9/177) of single CD38^{lo} luminal cells were capable of generating organoids (Figure 2F), which is considerably greater than the rate of CD38^{hi} luminal cells (1/142) and the 1% rate reported for CD26^{+} luminal cells (Karthaus et al., 2014; Park et al., 2016).

CD38^{lo} Luminal Cells Exhibit an Inflammatory Signature

To investigate potential mechanisms regulating differential progenitor activity, we performed RNA sequencing (RNA-seq) and microarray analysis. We generated an RNA-seq signature comprised of 449 genes greater than 2 fold-enriched in CD38^{lo} luminal cells compared to CD38^{hi} luminal cells and greater than 1.5-fold enriched compared to basal cells (Table S1). We found that CD38^{lo} luminal cells express elevated levels of BCL2, a gene previously associated with PIA (De Marzo et al., 1999) (Figure 3A). A number of inflammatory-related genes including cytokines (*Tnf*, *Il6*, and *Il8*) and chemokines (*Cxcl1*, *Cxcl2*, *Cxcl3*, *Cxcl6*, *Ccl2*, and *Ccl20*) are enriched in CD38^{lo} luminal cells (Figure 3A). We performed pathway analysis using DAVID Bioinformatics (Huang da et al., 2009) and found the most significant keywords included “inflammatory signaling” and “immune response” (Figure 3B). The significant pathways and inflammatory-related genes were confirmed to be upregulated in CD38^{lo} luminal cells by microarray analysis. We confirmed activation of the nuclear factor κB (NF-κB) pathway at the protein level based on phosphorylated p65 and expression of BCL2 by western blot (Figure 3C). In tissue sections, we found that phosphorylated p65 was highly expressed in CD38^{lo} luminal cells in a pattern inversely correlated with CD38 (Figure 3D). Ingenuity pathway analysis identified tumor necrosis factor alpha (TNF) as a likely upstream regulator of CD38^{lo} luminal cells. We confirmed that TNF is expressed in CD38^{lo} cells but absent from CD38^{hi} luminal cells by immunohistochemistry (Figure S3A), suggesting that TNF may activate NFkB signaling in CD38^{lo} cells. We observed a diminution of p65 phosphorylation and reduced expression of BCL2 in CD38^{lo} cells following treatment with the NF-κB pathway inhibitor ACHP (Figure S3B). In a functional assay, ACHP treatment blocked the organoid-forming progenitor activity of CD38^{lo} luminal cells to a greater extent than other epithelial subsets (Figure S3C).

Author Manuscript Author Manuscript Author Manuscript Author Manuscript

CD38^{lo} Luminal Cells Are Expanded in Glands Adjacent to Inflammation

Based on their gene expression profiling, including genes associated with PIA and inflammation, we investigated expression of CD38 in regions containing inflammatory infiltration (Figure 3E). Staining for CD38 and CD45 on serial slides indicates that CD38 expression is reduced adjacent to CD45$^+$ cells (Figure 3F). We stained for a panel of immune cell subsets and found evidence of CD4$^+$ and CD8$^+$ T cells, CD11c$^+$ and CD68$^+$ myeloid cells, and CD20$^+$ B cells adjacent to regions of the gland with low expression of CD38 (Figure S3D). In order to better define the relationship between CD38 expression and inflammation, we stratified glands into three categories: normal, inflamed, and atrophic, as classified by an expert pathologist. Inflamed glands were identified by pathologic criteria and confirmed with CD45 staining. Atrophic glands were identified by pathologic criteria and generally measured less than 20 μm from the basement membrane to the lumen in contrast to normal glands (Figure S3E). Loss of CD38 expression was measured in 95% (38/40) of inflamed glands, 88% (35/40) of atrophic glands, and only 10% (4/40) of normal glands from representative patient samples. Similar results were obtained for TNF, with strong expression in inflamed (38/40) and atrophic glands (33/40) with rare expression in normal glands (1/40). We further explored the connection between immune cells and CD38^{lo} luminal cells by flow cytometry in benign human prostate tissues from 29 distinct patient samples. We found a statistically significant association between the percentage of CD45$^+$ immune cells and the proportion of luminal cells exhibiting a CD38^{lo} surface phenotype (Figures 3G and S3F).

Reduced Androgen Signaling in CD38^{lo} Luminal Cells

CD38^{lo} luminal cells express lower levels of *Klk3*, the gene for prostate-specific antigen (PSA) and other androgen-target genes (*Klk2*, *Klk4*, *Msmb*, *Acpp*, and *Fkbp5*) (Figure 3A), consistent with reduced androgen signaling observed in PIA lesions (De Marzo et al., 1999). Similar results were observed by microarray analysis. qPCR confirmed differences in *Klk3* mRNA between the luminal subsets (Figure 4A). In contrast, levels of the luminal gene K8 were not significantly different (Figure 4A). Using immunohistochemistry, we confirmed diminished expression of androgen targets PSA, FKBP5, and MSMB in CD38^{lo} luminal cells at the protein level (Figure 4B). Androgen receptor (AR) target NKX3-1 was also reduced in CD38^{lo} luminal cells (Figure S4). We hypothesized that low androgen signaling in CD38^{lo} luminal cells may be due to low levels of AR. While AR is expressed in CD38^{lo} cells, protein levels are reduced compared to CD38^{hi} luminal cells (Figures 1E and 4C).

CD38^{lo} Luminal Phenotype Is Associated with Disease Progression and Poor Outcome

CD38 expression was previously reported to be reduced in a small cohort of prostate cancer specimens compared to benign prostate tissues (Kramer et al., 1995). We examined expression of CD38 in a tissue microarray containing tissue cores from 267 patients with prostate cancer (Gollapudi et al., 2013) (Table S2) and found the highest protein expression of CD38 in benign glands, with reduced expression in PIN and prostate cancer (Figures 5A and 5B; Table S3). The lowest expression of CD38 was found in the most advanced tumors based on Gleason grade (Figures 5A and 5B). Immunohistochemical staining was verified using two different anti-CD38 antibodies (Figure S5). While the average CD38 expression

Author Manuscript Author Manuscript Author Manuscript Author Manuscript

level was statistically significantly associated with time to biochemical recurrence, CD38 expression in cancer specimens was not statistically significant (Table S4).

Using the Memorial Sloan Kettering Cancer Center (MSKCC) dataset (Hieronymus et al., 2014; Taylor et al., 2010), we found that low CD38 mRNA in prostatectomy-derived prostate cancer samples is prognostic for biochemical recurrence and metastasis (Figures 5C and 5D) in a statistically significant manner (Table S5). Importantly, low CD38 mRNA status is statistically significantly associated with both biochemical recurrence and metastasis after correction for Stephenson nomogram score (Stephenson et al., 2005), which includes both clinical and pathological variables (Table S5). Low CD38 mRNA is also prognostic for biochemical recurrence in the Cancer Genome Atlas (TCGA) dataset (Network, 2015) (Figure 5E). Upon stratifying tumors based on genotype, we found that low CD38 mRNA expression was associated with SPINK1 outlier status, but not ETS-related gene (ERG) rearrangements, in the MSKCC cohort (Figure S6A).

To determine whether the $CD38^{lo}$ luminal gene signature could provide value in predicting patient survival, we turned to a Swedish watchful waiting cohort containing outcome data for 281 men (Sboner et al., 2010). The mean of the scaled expression values of the $CD38^{lo}$ luminal genes was significantly ($p = 0.037$) associated with all-cause mortality after adjusting for Gleason sum, age, and cancer percentage (Table S6A). When we analyzed the patients most at risk for prostate cancer-related mortality, with a Gleason score greater than or equal to 7 and follow-up within 5 years, we found a statistically significant difference ($p = 0.007$) between patients whose expression values lie in the top third ($CD38^{lo}$ luminal-like) versus all others (Figure S6B; Table S6C). The statistical significance of the $CD38^{lo}$ signature within this restricted group reached $p = 0.0007$ after adjusting for Gleason sum, age, and cancer percentage (Table S6B). The $CD38^{lo}$ luminal gene signature is inversely correlated with the AR signature score (Hieronymus et al., 2006) in prostate tumor specimens in a statistically significant manner in multiple cohorts (Figure S6C). We confirmed that the effect of the $CD38^{lo}$ signature was independent of the AR signature (Hieronymus et al., 2006; Nelson et al., 2002) and a previously reported immune signature (Jin et al., 2014) (Tables S6D and S6E).

$CD38^{lo}$ Luminal Cells Express the Therapeutic Target PSCA

While CD38 expression is low in the most aggressive tumors, we reasoned that genes in the $CD38^{lo}$ luminal cell signature may be expressed in advanced disease and might serve as positive markers of this cell population. We used immunohistochemistry to investigate expression of prostate stem cell antigen (PSCA), a therapeutic target expressed in aggressive, metastatic, and castration-resistant prostate cancer (Gu et al., 2000). *Psca* is enriched in $CD38^{lo}$ cells (Figure 3A) but has not been previously associated with PIA. In tissue sections, PSCA expression was observed more commonly in inflamed (28/40) glands than atrophic (15/40) or benign (12/40) glands, in an expression pattern inversely correlated with CD38 (Figure 6A). In some regions, these two markers can distinguish benign glands ($CD38^{hi}$ PSCA-low) from cancer ($CD38^{lo}$ PSCA-hi) (Figure 6B). We hypothesized that $CD38^{lo}$ PSCA-hi cancers may arise from the transformation of $CD38^{lo}$ PSCA-hi luminal cells.

Author Manuscript Author Manuscript Author Manuscript Author Manuscript

CD38^{lo} Luminal Cells Can Regenerate Glands and Initiate Human Prostate Cancer

To determine the functional capacity of CD38^{lo} luminal cells in tissue-regeneration and disease-initiation, we turned to an in vivo regeneration assay where human prostate epithelial cells are combined with urogenital sinus mesenchyme cells (UGSM) in Matrigel and transplanted subcutaneously into immune-deficient mice (Goldstein et al., 2010, 2011). To track human epithelial cells, we introduced genes for red and green fluorescent proteins into CD38^{lo} luminal cells prior to in vivo transplantation (Figures 7A and S7A). Due to low cell numbers insufficient for direct in vivo implantation, we utilized a recently published approach to expand isolated cells in organoid culture for 1–2 weeks prior to transplantation (Park et al., 2016). An average of 200 lentiviral-transduced organoids derived from CD38^{lo} luminal cells were combined with UGSM and implanted into NOD-SCID-IL2Rγ^{null} mice. 8 weeks post-transplantation, we identified prostatic glands containing both luminal cells expressing K8 and AR and basal cells expressing K5 and p63 (Figure 7B). Lentiviral transduced human epithelial structures in regenerated tissues could be identified based on fluorescent signal, whereas control grafts without human cells lacked any epithelial structures or fluorescence (Figure S7C).

Oncogenes previously shown to transform primary human prostate (Goldstein et al., 2010; Stoyanova et al., 2013) (Myc, myristoylated AKT, and AR) were introduced into double-sorted CD38^{lo} luminal cells via lentiviral delivery prior to in vitro expansion and in vivo transplantation. We identified features of human prostate adenocarcinoma, including expression of the luminal markers K8, PSA, and AR and an absence of the basal markers K5 and p63 in regenerated tumors derived from oncogene-expressing CD38^{lo} luminal cells (Figure 7C). Regenerated tumors exhibited expression of oncogenes (Figure S7B). Importantly, tumors exhibited the PSCA-hi CD38^{lo} luminal phenotype and a high frequency of cells expressed the proliferative marker Ki67 (>40% Ki67^{+}) (Figure 7C). Results were confirmed using tissue from four independent patient samples. These findings indicate that CD38^{lo} luminal cells can initiate human prostate cancer in vivo.

DISCUSSION

Chronic inflammation is associated with cancer initiation, progression, metastasis, and treatment resistance in a range of tumor types including prostate cancer (Das Roy et al., 2009; Gurel et al., 2014; Liu et al., 2013; Wang et al., 2015). In mouse models, several groups have established a tumor-promoting functional contribution of distinct immune cell types to prostate cancer, including B cells and myeloid-derived suppressor cells (Ammirante et al., 2010; Garcia et al., 2014). However, little is known about the influence of inflammation on the function of human prostate epithelium prior to tumor formation. De Marzo and colleagues have proposed that inflammation may be an inciting event in prostate transformation and that PIA cells may serve as target cells for tumor initiation (De Marzo et al., 1999, 2003, 2007). Our results demonstrate that PIA-like CD38^{lo} luminal cells can initiate human prostate cancer.

Several groups have isolated human prostate luminal cells based on low expression of CD49f or high expression of CD26 for functional studies (Goldstein et al., 2010; Karthaus et al., 2014; Park et al., 2016; Stoyanova et al., 2013). We found that CD26 and CD38 identify

Author Manuscript Author Manuscript Author Manuscript Author Manuscript

an analogous population of prostate luminal cells (Figure S1C). While rare cells within the $CD26^{+}$ or $CD38^{hi}$ luminal cell population exhibit organoid-forming activity, ~99% of cells in this subset do not exhibit progenitor features (Figures 2B–2D; Karthaus et al., 2014; Park et al., 2016). In contrast, $CD38^{lo}$ luminal cells are enriched for progenitor activity in 2D and 3D progenitor assays, as 5% of $CD38^{lo}$ luminal cells are capable of generating organoids (Figure 2D), similar to the rate of *Lgr5*-GFP-hi intestinal stem cells (Sato et al., 2009). Therefore, identifying the signaling pathways active in $CD38^{lo}$ luminal cells may yield mechanisms regulating luminal progenitor activity.

We found that $CD38^{lo}$ and $CD38^{hi}$ luminal cells have distinct transcriptional signatures. While androgen signaling is active in $CD38^{hi}$ luminal cells (Figure 4), $CD38^{lo}$ luminal cells exhibit elevated NF-κB signaling (Figure 3). Previous studies demonstrate that NF-κB activation can synergize with MYC overexpression or *Pten* heterozygosity to accelerate murine prostate cancer initiation and the NF-κB activation signature in human tumors can predict poor outcome (Birbach et al., 2011; Jin et al., 2014). These data suggest that NF-κB activity may predispose $CD38^{lo}$ luminal cells to tumor initiation. More work is necessary to determine whether strategies to reduce inflammation or small molecules that block epithelial NF-κB signaling can prevent prostate cancer initiation by targeting $CD38^{lo}$ luminal cell survival and progenitor activity.

$CD38^{lo}$ luminal cells express PSCA, which is being evaluated as a therapeutic target in clinical trials using monoclonal antibodies (Morris et al., 2012). BCL2 expression in $CD38^{lo}$ luminal cells may enhance their resistance to apoptosis (Raffo et al., 1995). Both BCL2 and PSCA are associated with castration resistance (Gu et al., 2000; Raffo et al., 1995), suggesting that $CD38^{lo}$ luminal cells may have a survival advantage under low-androgen conditions. Consistent with mouse models demonstrating that prostatic inflammation or epithelial NF-κB activation is associated with reduced androgen signaling and increased epithelial proliferation (Birbach et al., 2011; Khalili et al., 2010), $CD38^{lo}$ luminal cells express low levels of PSA and other androgen targets. These data suggest that $CD38^{lo}$ luminal-like cancer cells may contribute to castration-resistant prostate cancer.

Distinguishing indolent from aggressive prostate cancer remains a critical goal of the field. We found that low expression of CD38 mRNA in prostatectomy specimens is prognostic for biochemical recurrence in two independent cohorts (Figures 5C–5E). These data suggest that aggressive tumors may arise in $CD38^{lo}$ luminal cells that retain low expression of CD38. Alternatively, the activation of a $CD38^{lo}$ luminal-like signature during tumorigenesis may promote an aggressive phenotype, regardless of the cell of origin. Several studies have looked at the cellular origins of cancer to distinguish indolent from aggressive prostate cancer with different results using distinct mouse models (Choi et al., 2012; Lu et al., 2013; Wang et al., 2009, 2013, 2014). In human prostate models, basal cells have been shown to generate aggressive, highly proliferative tumors, while luminal cells can initiate only indolent tumors (Goldstein et al., 2010; Park et al., 2016; Stoyanova et al., 2013). In this study, we demonstrate that $CD38^{lo}$ luminal cells can generate highly proliferative prostate cancer (>40% Ki67+). Taken together, we hypothesize that one target cell (basal) is predisposed to the initiation of aggressive cancer under normal conditions. In the context of

Author Manuscript Author Manuscript Author Manuscript Author Manuscript

chronic inflammation, a second target cell (CD38^{lo} luminal) is predisposed to initiate aggressive cancer, perhaps due to elevated NF-κB signaling.

CD38^{lo} luminal cells may arise from basal to luminal differentiation, as has been demonstrated using lineage tracing in mouse models of inflammation (Kwon et al., 2014, 2016). Alternatively, inflammation may alter the differentiation of luminal cells by enhancing NF-κB signaling and reducing androgen signaling. Future studies will determine whether exposure to inflammatory cytokines can reprogram CD38^{hi} luminal cells into a progenitor-enriched CD38^{lo} luminal-like cell capable of initiating aggressive prostate cancer. Interestingly, CD38^{lo} luminal cells express cytokines and chemokines known to recruit pro-inflammatory cells and promote tumorigenesis in other tissues like *Ccl2* (Qian et al., 2011) and *Cxcl1/2* (Jablonska et al., 2014), indicating that CD38^{lo} luminal cells may influence their microenvironment to promote inflammation and maintain proliferative cues.

Our findings are consistent with previous reports of low CD38 expression in prostate cancer (Kramer et al., 1995; Pascal et al., 2009). While rare deletions and mutations of CD38 can be identified in metastatic castration-resistant prostate cancer (Grasso et al., 2012; Robinson et al., 2015), transcriptional repression of CD38 is the likely mechanism causing low expression in the vast majority of prostate tumors. CD38 is an ectoenzyme that consumes the cofactor nicotinamide adenine dinucleotide (NAD) (Howard et al., 1993), suggesting that loss of CD38 may serve to increase pools of NAD required for cellular metabolism in prostate cancer. Further study of the functional role of CD38 in tumorigenesis and the cellular mechanisms driving CD38^{lo} luminal cells may yield new predictive markers and therapeutic targets for aggressive disease.

EXPERIMENTAL PROCEDURES

qPCR, RNA Sequencing, Bioinformatics, and Microarray

RNA was extracted from cell pellets using the RNeasy mini Kit (QIAGEN/SA Biosciences). qPCR was carried out as previously described (Goldstein et al., 2010) using commercial primers to *Gapdh*, *Keratin 8*, and *Klk3* (QIAGEN/SA Biosciences). RNA-seq libraries were prepared with the Ovation RNA-Seq System V2 (Nugen). Double-stranded cDNA was generated with a mixture of random and poly(T) priming, followed by fragmentation, generation of blunt ends by end repair, A-tailing, ligation of adaptors (different adaptors for multiplexing samples), PCR amplification, and sequencing (pair read 100 run) on Illumina HiSeq 2500. Illumina SAV was used for data quality check, and Illumina CASAVA 1.8.2 was used for de-multiplexing. Reads were mapped to the most recent UCSC transcript set with Bowtie2 version 2.1.0. RSEM v1.2.15 was used to estimate level of gene expression. Gene expression was normalized by TPM (transcript per million) or RPKM (reads per kilobase per million mapped reads). DeSeq was used to identify differentially expressed genes. FASTQ files were not available at the time of publication. For that reason, the full RPKM values are provided in Table S1. Upstream regulator analysis was performed using QIAGEN's Ingenuity Pathway Analysis (http://www.ingenuity.com). For microarray analysis, total RNA was isolated from sorted cells with RNeasy Micro Kit and amplified with NuGen Pico kit according to standard manufacturer protocols. Biotinylated cDNA were prepared from total RNA using the standard Affymetrix protocol and hybridized to the

Author Manuscript Author Manuscript Author Manuscript Author Manuscript

Affymetrix Human Genome U133 Plus 2.0 Chip. Chips were scanned using an Affymetrix GeneChip Scanner 7G and data were analyzed with Microarray Suite version 5.0 (MAS 5.0) using Affymetrix default analysis settings and global scaling as normalization method. Data are available at the GEO repository under accession number GEO: GSE89050.

Primary Cell Preparation and Cell Separation

Human prostate tissue samples were provided in a de-identified manner deemed by the institutional review board to not qualify as human subjects. Tissue was provided by the UCLA Translational Pathology Core Laboratory, and benign specimens were processed as described in detail previously (Goldstein et al., 2011). For antibody staining of primary benign dissociated cells, see Supplemental Information). Intracellular flow cytometry has been described previously (Goldstein et al., 2010). Antibodies are listed in Supplemental Information.

Immunohistochemical Analysis and Immunofluorescence

Paraffin-embedded tissue sections were incubated in a 60°C oven for 1 hr and de-paraffinized in three changes of xylene, followed by 100% alcohol twice for 3 min each. Then the slides were transferred once in 95% and 70% alcohol, each for 3 min. A heat antigen retrieval step was used to unmask the antigenic epitopes. The remaining procedure was performed according to the manufacturer's protocol (R&D Cell and Tissue Staining Kit HRP-DAB system, R&D Systems). Primary antibodies are listed in Supplemental Information. Biotinylated anti-mouse and anti-rabbit secondary antibodies are supplied by HRP-DAB system for Mouse (CTS002, R&D Systems) and Rabbit Kit (CTS005, R&D Systems). Double-sorted cells were plated onto a glass slide coated with poly-L-lysine (Sigma), and cells were allowed to attach overnight. The following day, cells were fixed in 4% paraformaldehyde, washed three times in 1× PBS and stained with primary antibody. Alexa-488-conjugated goat anti-mouse secondary antibody (A-11001, Invitrogen) was used followed by DAPI nuclear counterstain (H-1200, Vector Laboratories).

Immunoblot Analysis

Isolated cell populations were lysed in RIPA buffer (150mM NaCl, 1% NP-40, 50 mM Tris-HCl [pH 8.0], 0.5% sodium deoxycholate, and 0.1% SDS) with protease inhibitor cocktail tablet (Complete, Roche) on ice 15 min followed by spin at maximum speed for 15 min. Supernatants were boiled in loading buffer and membranes probed with antibodies (see Supplemental Information). Primary rabbit, mouse, or goat antibodies were detected with horseradish peroxidase (HRP)-conjugated secondary antibodies (Pierce).

Tissue Microarray and Scoring

The tissue microarray was constructed from 332 men who underwent radical prostatectomy surgery at the West Los Angeles Veteran's Administration Hospital from 1991 to 2003 and has been described previously (Gollapudi et al., 2013). At least three cores of each histological type are included per patient. Follow-up patient information for up to 120 months was used for analysis. Biochemical recurrence refers to PSA values greater than 0.2, two readings at 0.2, or additional treatment for high post-operative PSA. 4-μm sections were

Author Manuscript Author Manuscript Author Manuscript Author Manuscript

stained for CD38 and scanned using the Aperioslide scanner, and staining was evaluated in a blinded fashion by the pathologists (B.N. and J.H.). Scoring was assessed based on staining intensity from 0 (no staining) to 3 (strong) and percentage of tumor cell expression (1%–100%), creating a composite score from 0 to 300. For statistical methods, see Supplemental Information.

Cell Culture

For the in vitro organoid-forming assay, double-sorted FACS-isolated cell populations were plated in a 96-well plate (Corning Incorporated) at a cell density of one cell per well, and those wells with a single cell were visually confirmed and marked for continued analysis. Prostate organoid growth conditions were based on established protocols (Karthaus et al., 2014). Primary single-cell organoids were dissociated in 1 mg/mL Dispase (Gibco) at 37°C for 1 hr and then treated with 0.05% Trypsin-EDTA (Life Technologies) in order to passage. For the colony assay, primary cells were plated on Matrigel-coated six-well dishes as described previously (Lukacs et al., 2010) and grown in PrEGM media. Colonies containing more than two cells were quantified after 10–14 days. For the sphere assay, cells were resuspended in a PrEGM/Matrigel mixture and plated around the edges of the well in a 12-well dish as described previously (Lukacs et al., 2010). Spheres were quantified after 10–14 days. For inhibition of NF-κB, ACHP (4547, Tocris) was added to organoid media at a final concentration of 5 μM every 3 days.

In Vivo Regeneration and Transformation and Animal Care

In vivo tissue-regeneration and transformation methods have been described in detail (Goldstein et al., 2011). Transduced cells were expanded in organoid culture (Karthaus et al., 2014) prior to transplantation as described previously (Park et al., 2016). All human tissues were transplanted subcutaneously into NOD-SCID-IL2Rγ^{null} mice. Animals have been purchased from the Jackson Laboratory and are now housed and bred under the care of the Division of Laboratory Animal Medicine at the University of California, Los Angeles, using protocols approved by the Animal Research Committee. Lentiviral vectors were previously described (Goldstein et al., 2010; Stoyanova et al., 2013).

Supplementary Material

Refer to Web version on PubMed Central for supplementary material.

Acknowledgments

This work was supported by Department of Defense Idea Development Award W81XWH-13-1-0470 (A.S.G. and S.H.), a Prostate Cancer Foundation Young Investigator Award (A.S.G. and T.S.), the Broad Stem Cell Research Center (A.S.G. and J.H.), an AACR/PCF/Stand Up 2 Cancer West Coast Dream Team Award (O.N.W., J.H., M.R., and A.S.G.), a National Institute of Health/National Cancer Institute grant (P50CA092131/UCLA SPORE in Prostate Cancer; D.E., S.H., O.N.W., J.H., M.R., and A.S.G), a NIH/National Center for Advancing Translational Science (NCATS) UCLA CTSI grant (UL1TR000124; T.R.G. and D.E.), a National Institute of Health/National Cancer Institute K99 Pathway to Independence Award (4R00CA184397; T.S.), and the Howard Hughes Medical Institute (O.N.W.). M.R. and funding for TMA creation were supported by the Department of Defense (PC030686).

Author Manuscript Author Manuscript Author Manuscript Author Manuscript

References

Ammirante M, Luo JL, Grivennikov S, Nedospasov S, Karin M. B-cell-derived lymphotoxin promotes castration-resistant prostate cancer. Nature. 2010; 464:302–305. [PubMed: 20220849]

Birbach A, Eisenbarth D, Kozakowski N, Ladenhauf E, Schmidt-Supprian M, Schmid JA. Persistent inflammation leads to proliferative neoplasia and loss of smooth muscle cells in a prostate tumor model. Neoplasia. 2011; 13:692–703. [PubMed: 21847361]

Choi N, Zhang B, Zhang L, Ittmann M, Xin L. Adult murine prostate basal and luminal cells are self-sustained lineages that can both serve as targets for prostate cancer initiation. Cancer Cell. 2012; 21:253–265. [PubMed: 22340597]

Coussens LM, Werb Z. Inflammation and cancer. Nature. 2002; 420:860–867. [PubMed: 12490959]

Das Roy L, Pathangey LB, Tinder TL, Schettini JL, Gruber HE, Mukherjee P. Breast-cancer-associated metastasis is significantly increased in a model of autoimmune arthritis. Breast Cancer Res. 2009; 11:R56. [PubMed: 19643025]

De Marzo AM, Marchi VL, Epstein JI, Nelson WG. Proliferative inflammatory atrophy of the prostate: implications for prostatic carcinogenesis. Am J Pathol. 1999; 155:1985–1992. [PubMed: 10595928]

De Marzo AM, Meeker AK, Zha S, Luo J, Nakayama M, Platz EA, Isaacs WB, Nelson WG. Human prostate cancer precursors and pathobiology. Urology. 2003; 62(5, Suppl 1):55–62.

De Marzo AM, Platz EA, Sutcliffe S, Xu J, Grönberg H, Drake CG, Nakai Y, Isaacs WB, Nelson WG. Inflammation in prostate carcinogenesis. Nat Rev Cancer. 2007; 7:256–269. [PubMed: 17384581]

Elkahwaji JE, Hauke RJ, Brawner CM. Chronic bacterial inflammation induces prostatic intraepithelial neoplasia in mouse prostate. Br J Cancer. 2009; 101:1740–1748. [PubMed: 19844236]

Garcia AJ, Ruscetti M, Arenzana TL, Tran LM, Bianci-Frias D, Sybert E, Priceman SJ, Wu L, Nelson PS, Smale ST, Wu H. Pten null prostate epithelium promotes localized myeloid-derived suppressor cell expansion and immune suppression during tumor initiation and progression. Mol Cell Biol. 2014; 34:2017–2028. [PubMed: 24662052]

Goldstein AS, Lawson DA, Cheng D, Sun W, Garraway IP, Witte ON. Trop2 identifies a subpopulation of murine and human prostate basal cells with stem cell characteristics. Proc Natl Acad Sci USA. 2008; 105:20882–20887. [PubMed: 19088204]

Goldstein AS, Huang J, Guo C, Garraway IP, Witte ON. Identification of a cell of origin for human prostate cancer. Science. 2010; 329:568–571. [PubMed: 20671189]

Goldstein AS, Drake JM, Burnes DL, Finley DS, Zhang H, Reiter RE, Huang J, Witte ON. Purification and direct transformation of epithelial progenitor cells from primary human prostate. Nat Protoc. 2011; 6:656–667. [PubMed: 21527922]

Gollapudi K, Galet C, Grogan T, Zhang H, Said JW, Huang J, Elashoff D, Freedland SJ, Rettig M, Aronson WJ. Association between tumor-associated macrophage infiltration, high grade prostate cancer, and biochemical recurrence after radical prostatectomy. Am J Cancer Res. 2013; 3:523–529. [PubMed: 24224130]

Grasso CS, Wu YM, Robinson DR, Cao X, Dhanasekaran SM, Khan AP, Quist MJ, Jing X, Lonigro RJ, Brenner JC, et al. The mutational landscape of lethal castration-resistant prostate cancer. Nature. 2012; 487:239–243. [PubMed: 22722839]

Gu Z, Thomas G, Yamashiro J, Shintaku IP, Dorey F, Raitano A, Witte ON, Said JW, Loda M, Reiter RE. Prostate stem cell antigen (PSCA) expression increases with high gleason score, advanced stage and bone metastasis in prostate cancer. Oncogene. 2000; 19:1288–1296. [PubMed: 10713670]

Gurel B, Lucia MS, Thompson IM Jr, Goodman PJ, Tangen CM, Kristal AR, Parnes HL, Hoque A, Lippman SM, Sutcliffe S, et al. Chronic inflammation in benign prostate tissue is associated with high-grade prostate cancer in the placebo arm of the prostate cancer prevention trial. Cancer Epidemiol Biomarkers Prev. 2014; 23:847–856. [PubMed: 24748218]

Haverkamp JM, Charbonneau B, Crist SA, Meyerholz DK, Cohen MB, Snyder PW, Svensson RU, Henry MD, Wang HH, Ratliff TL. An inducible model of abacterial prostatitis induces antigen specific inflammatory and proliferative changes in the murine prostate. Prostate. 2011; 71:1139–1150. [PubMed: 21656824]

Author Manuscript Author Manuscript Author Manuscript Author Manuscript

Hieronymus H, Lamb J, Ross KN, Peng XP, Clement C, Rodina A, Nieto M, Du J, Stegmaier K, Raj SM, et al. Gene expression signature-based chemical genomic prediction identifies a novel class of HSP90 pathway modulators. Cancer Cell. 2006; 10:321–330. [PubMed: 17010675]

Hieronymus H, Schultz N, Gopalan A, Carver BS, Chang MT, Xiao Y, Heguy A, Huberman K, Bernstein M, Assel M, et al. Copy number alteration burden predicts prostate cancer relapse. Proc Natl Acad Sci USA. 2014; 111:11139–11144. [PubMed: 25024180]

Howard M, Grimaldi JC, Bazan JF, Lund FE, Santos-Argumedo L, Parkhouse RM, Walseth TF, Lee HC. Formation and hydrolysis of cyclic ADP-ribose catalyzed by lymphocyte antigen CD38. Science. 1993; 262:1056–1059. [PubMed: 8235624]

Huang da W, Sherman BT, Lempicki RA. Systematic and integrative analysis of large gene lists using DAVID bioinformatics resources. Nat Protoc. 2009; 4:44–57. [PubMed: 19131956]

Jablonska J, Wu CF, Andzinski L, Leschner S, Weiss S. CXCR2-mediated tumor-associated neutrophil recruitment is regulated by IFN-β. Int J Cancer. 2014; 134:1346–1358. [PubMed: 24154944]

Jin R, Yi Y, Yull FE, Blackwell TS, Clark PE, Koyama T, Smith JA Jr, Matusik RJ. NF-κB gene signature predicts prostate cancer progression. Cancer Res. 2014; 74:2763–2772. [PubMed: 24686169]

Karthaus WR, Iaquinta PJ, Drost J, Gracanin A, van Boxtel R, Wongvipat J, Dowling CM, Gao D, Begthel H, Sachs N, et al. Identification of multipotent luminal progenitor cells in human prostate organoid cultures. Cell. 2014; 159:163–175. [PubMed: 25201529]

Khalili M, Mutton LN, Gurel B, Hicks JL, De Marzo AM, Bieberich CJ. Loss of Nkx3.1 expression in bacterial prostatitis: a potential link between inflammation and neoplasia. Am J Pathol. 2010; 176:2259–2268. [PubMed: 20363913]

Kramer G, Steiner G, Födinger D, Fiebiger E, Rappersberger C, Binder S, Hofbauer J, Marberger M. High expression of a CD38-like molecule in normal prostatic epithelium and its differential loss in benign and malignant disease. J Urol. 1995; 154:1636–1641. [PubMed: 7563309]

Kwon OJ, Zhang L, Ittmann MM, Xin L. Prostatic inflammation enhances basal-to-luminal differentiation and accelerates initiation of prostate cancer with a basal cell origin. Proc Natl Acad Sci USA. 2014; 111:E592–E600. [PubMed: 24367088]

Kwon OJ, Zhang B, Zhang L, Xin L. High fat diet promotes prostatic basal-to-luminal differentiation and accelerates initiation of prostate epithelial hyperplasia originated from basal cells. Stem Cell Res (Amst). 2016; 16:682–691.

Lawson DA, Zong Y, Memarzadeh S, Xin L, Huang J, Witte ON. Basal epithelial stem cells are efficient targets for prostate cancer initiation. Proc Natl Acad Sci USA. 2010; 107:2610–2615. [PubMed: 20133806]

Liu K, Jiang M, Lu Y, Chen H, Sun J, Wu S, Ku WY, Nakagawa H, Kita Y, Natsugoe S, et al. Sox2 cooperates with inflammation-mediated Stat3 activation in the malignant transformation of foregut basal progenitor cells. Cell Stem Cell. 2013; 12:304–315. [PubMed: 23472872]

Lu TL, Huang YF, You LR, Chao NC, Su FY, Chang JL, Chen CM. Conditionally ablated Pten in prostate basal cells promotes basal-to-luminal differentiation and causes invasive prostate cancer in mice. Am J Pathol. 2013; 182:975–991. [PubMed: 23313138]

Lukacs RU, Goldstein AS, Lawson DA, Cheng D, Witte ON. Isolation, cultivation and characterization of adult murine prostate stem cells. Nat Protoc. 2010; 5:702–713. [PubMed: 20360765]

Morris MJ, Eisenberger MA, Pili R, Denmeade SR, Rathkopf D, Slovin SF, Farrelly J, Chudow JJ, Vincent M, Scher HI, Carducci MA. A phase I/IIA study of AGS-PSCA for castration-resistant prostate cancer. Ann Oncol. 2012; 23:2714–2719. [PubMed: 22553195]

Nelson PS, Clegg N, Arnold H, Ferguson C, Bonham M, White J, Hood L, Lin B. The program of androgen-responsive genes in neoplastic prostate epithelium. Proc Natl Acad Sci USA. 2002; 99:11890–11895. [PubMed: 12185249]

Network TR. Cancer Genome Atlas Research Network. The molecular taxonomy of primary prostate cancer. Cell. 2015; 163:1011–1025. [PubMed: 26544944]

Park JW, Lee JK, Phillips JW, Huang P, Cheng D, Huang J, Witte ON. Prostate epithelial cell of origin determines cancer differentiation state in an organoid transformation assay. Proc Natl Acad Sci USA. 2016; 113:4482–4487. [PubMed: 27044116]

Author Manuscript Author Manuscript Author Manuscript Author Manuscript

Pascal LE, Vêncio RZ, Page LS, Liebeskind ES, Shadle CP, Troisch P, Marzolf B, True LD, Hood LE, Liu AY. Gene expression relationship between prostate cancer cells of Gleason 3, 4 and normal epithelial cells as revealed by cell type-specific transcriptomes. BMC Cancer. 2009; 9:452. [PubMed: 20021671]

Qian BZ, Li J, Zhang H, Kitamura T, Zhang J, Campion LR, Kaiser EA, Snyder LA, Pollard JW. CCL2 recruits inflammatory monocytes to facilitate breast-tumour metastasis. Nature. 2011; 475:222–225. [PubMed: 21654748]

Raffo AJ, Perlman H, Chen MW, Day ML, Streitman JS, Buttyan R. Overexpression of bcl-2 protects prostate cancer cells from apoptosis in vitro and confers resistance to androgen depletion in vivo. Cancer Res. 1995; 55:4438–4445. [PubMed: 7671257]

Robinson D, Van Allen EM, Wu YM, Schultz N, Lonigro RJ, Mosquera JM, Montgomery B, Taplin ME, Pritchard CC, Attard G, et al. Integrative clinical genomics of advanced prostate cancer. Cell. 2015; 161:1215–1228. [PubMed: 26000489]

Sato T, Vries RG, Snippert HJ, van de Wetering M, Barker N, Stange DE, van Es JH, Abo A, Kujala P, Peters PJ, Clevers H. Single Lgr5 stem cells build crypt-villus structures in vitro without a mesenchymal niche. Nature. 2009; 459:262–265. [PubMed: 19329995]

Sboner A, Demichelis F, Calza S, Pawitan Y, Setlur SR, Hoshida Y, Perner S, Adami HO, Fall K, Mucci LA, et al. Molecular sampling of prostate cancer: a dilemma for predicting disease progression. BMC Med Genomics. 2010; 3:8. [PubMed: 20233430]

Sfanos KS, De Marzo AM. Prostate cancer and inflammation: the evidence. Histopathology. 2012; 60:199–215. [PubMed: 22212087]

Shafique K, Proctor MJ, McMillan DC, Qureshi K, Leung H, Morrison DS. Systemic inflammation and survival of patients with prostate cancer: evidence from the Glasgow Inflammation Outcome Study. Prostate Cancer Prostatic Dis. 2012; 15:195–201. [PubMed: 22343838]

Smith BA, Sokolov A, Uzunangelov V, Baertsch R, Newton Y, Graim K, Mathis C, Cheng D, Stuart JM, Witte ON. A basal stem cell signature identifies aggressive prostate cancer phenotypes. Proc Natl Acad Sci USA. 2015; 112:E6544–E6552. [PubMed: 26460041]

Stephenson AJ, Scardino PT, Eastham JA, Bianco FJ Jr, Dotan ZA, DiBlasio CJ, Reuther A, Klein EA, Kattan MW. Postoperative nomogram predicting the 10-year probability of prostate cancer recurrence after radical prostatectomy. J Clin Oncol. 2005; 23:7005–7012. [PubMed: 16192588]

Stoyanova T, Cooper AR, Drake JM, Liu X, Armstrong AJ, Pienta KJ, Zhang H, Kohn DB, Huang J, Witte ON, Goldstein AS. Prostate cancer originating in basal cells progresses to adenocarcinoma propagated by luminal-like cells. Proc Natl Acad Sci USA. 2013; 110:20111–20116. [PubMed: 24282295]

Taylor BS, Schultz N, Hieronymus H, Gopalan A, Xiao Y, Carver BS, Arora VK, Kaushik P, Cerami E, Reva B, et al. Integrative genomic profiling of human prostate cancer. Cancer Cell. 2010; 18:11–22. [PubMed: 20579941]

Taylor RA, Toivanen R, Frydenberg M, Pedersen J, Harewood L, Collins AT, Maitland NJ, Risbridger GP. Australian Prostate Cancer Bioresource. Human epithelial basal cells are cells of origin of prostate cancer, independent of CD133 status. Stem Cells. 2012; 30:1087–1096. [PubMed: 22593016]

van Leenders GJ, Gage WR, Hicks JL, van Balken B, Aalders TW, Schalken JA, De Marzo AM. Intermediate cells in human prostate epithelium are enriched in proliferative inflammatory atrophy. Am J Pathol. 2003; 162:1529–1537. [PubMed: 12707036]

Wang X, Kruithof-de Julio M, Economides KD, Walker D, Yu H, Halili MV, Hu YP, Price SM, Abate-Shen C, Shen MM. A luminal epithelial stem cell that is a cell of origin for prostate cancer. Nature. 2009; 461:495–500. [PubMed: 19741607]

Wang ZA, Mitrofanova A, Bergren SK, Abate-Shen C, Cardiff RD, Califano A, Shen MM. Lineage analysis of basal epithelial cells reveals their unexpected plasticity and supports a cell-of-origin model for prostate cancer heterogeneity. Nat Cell Biol. 2013; 15:274–283. [PubMed: 23434823]

Wang ZA, Toivanen R, Bergren SK, Chambon P, Shen MM. Luminal cells are favored as the cell of origin for prostate cancer. Cell Rep. 2014; 8:1339–1346. [PubMed: 25176651]

Wang D, Fu L, Sun H, Guo L, DuBois RN. Prostaglandin E2 promotes colorectal cancer stem cell expansion and metastasis in mice. Gastroenterology. 2015; 149:1884–1895. [PubMed: 26261008]

Author Manuscript Author Manuscript Author Manuscript Author Manuscript

Highlights

- Low expression of CD38 enriches for luminal progenitor cells in human prostate
- $CD38^{lo}$ luminal cells are localized in proximity to prostatic inflammation
- $CD38^{lo}$ luminal cells are target cells for aggressive human prostate cancer
- Low CD38 in prostate cancer is prognostic for biochemical recurrence and metastasis

Author Manuscript Author Manuscript Author Manuscript Author Manuscript

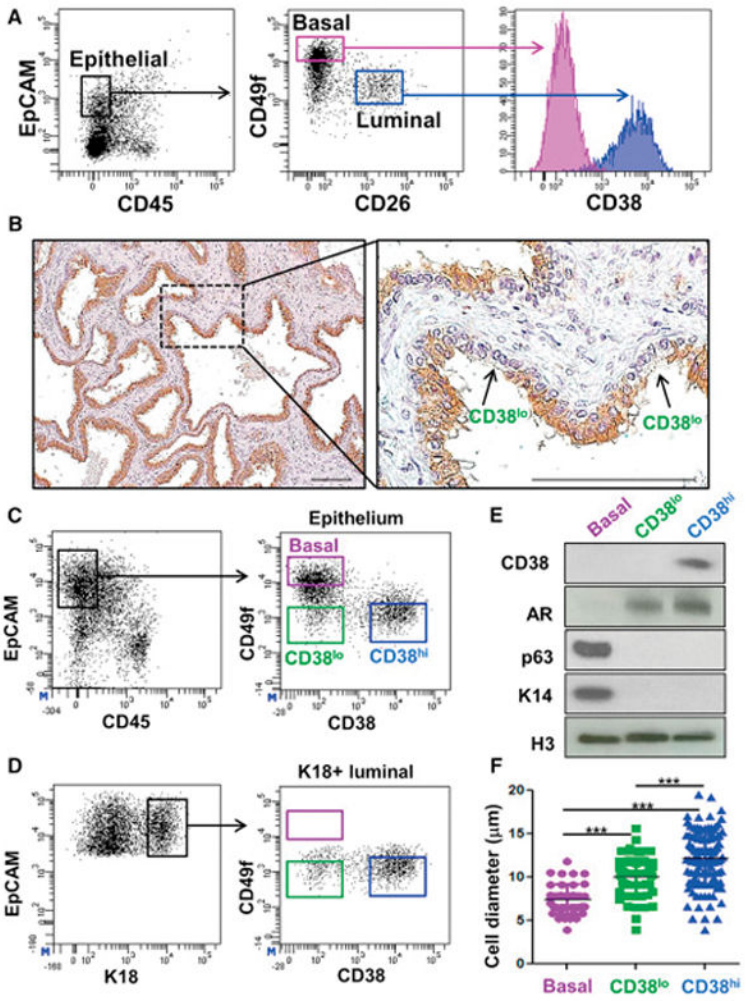

Figure 1. Differential Expression of CD38 Enables Isolation of Discrete Luminal Subsets from Fresh Human Prostate Tissue

(A) Fluorescence-activated cell sorting analysis of dissociated benign human prostate cells demonstrates CD38 expression in EpCAM^{+} CD45^{-} CD26^{+} luminal cells, but not in EpCAM^{+} CD45^{-} CD49f-hi basal cells.

(B) Immunohistochemical analysis of benign human prostate glands stained with anti-CD38 antibodies. Boxed region is magnified in the right. Arrows identify rare CD38^{lo} cells lining the gland. Scale bars, 50 μm.

(C) Fluorescence-activated cell sorting analysis of dissociated benign human prostate cells gated on EpCAM^{+} CD45^{-} cells and further stained with antibodies against CD49f and CD38.

(D) Intracellular flow cytometry for Keratin 18 (K18) and surface staining for CD38 and CD49f. Gating on K18^{+} luminal cells demonstrates two luminal populations in right plot.

(E) Western blot analysis of three epithelial subsets from representative patient sample stained with antibodies against CD38, AR, p63, keratin 14 (K14), and histone H3 as a loading control.

Author Manuscript Author Manuscript Author Manuscript Author Manuscript

(F) Sorted cells were counted in a hemocytometer, and average cell diameter (in microns) was quantified for each population from multiple patient samples.
Data represent mean ± SEM with replicate points shown. Newman-Keuls multiple comparison test with ***$p < 0.0001$.

Author Manuscript Author Manuscript Author Manuscript Author Manuscript

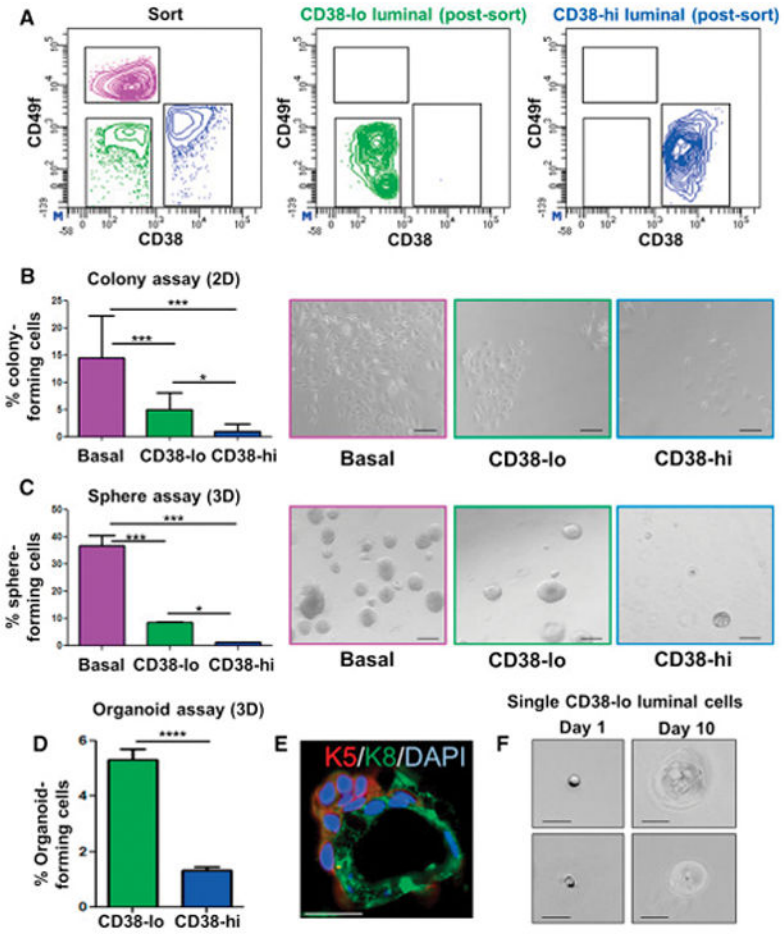

Figure 2. CD38^{lo} Cells Exhibit Greater Progenitor Activity than CD38^{hi} Luminal Cells In Vitro

(A) Flow cytometry analysis for CD49f and CD38 dissociated human prostate epithelium as gated during the sort (left), and post-sort analysis of CD38^{lo} and CD38^{hi} luminal cells prior to in vitro culture.

(B and C) Primary human benign prostate epithelial cells (EpCAM^{+} CD45^{-}) were sorted into basal cells, CD38^{lo} and CD38^{hi} luminal subsets and plated for in vitro colony and sphere forming assays. Results from in vitro two-dimensional colony-forming assay (B) and three-dimensional sphere-forming assay (C) measured 10–14 days after plating benign human prostate epithelial subsets. Data represent pooled experiments from three independent patients. Mean ± SEM is shown. Statistics represent Newman-Keuls multiple comparison test with *$p < 0.05$, ***$p < 0.0005$. Representative images of outgrowths from each epithelial subset are taken at 10–14 days. Scale bars, 250 μm.

(D) CD38^{lo} luminal cells generate significantly more organoids than CD38^{hi} luminal cells, four replicates per sample, representative of five independent patient samples. Statistics represent Two-tailed unpaired t test with ****$p < 0.0001$.

(E) Representative staining of CD38^{lo} luminal cell-derived organoids for K5, K8, and DAPI nuclear counterstain. Scale bars, 50 μm.

(F) Representative images of organoids forming from single CD38^{lo} luminal cells taken at day 1 and day 10. Scale bars, 100 μm.

Author Manuscript Author Manuscript Author Manuscript Author Manuscript

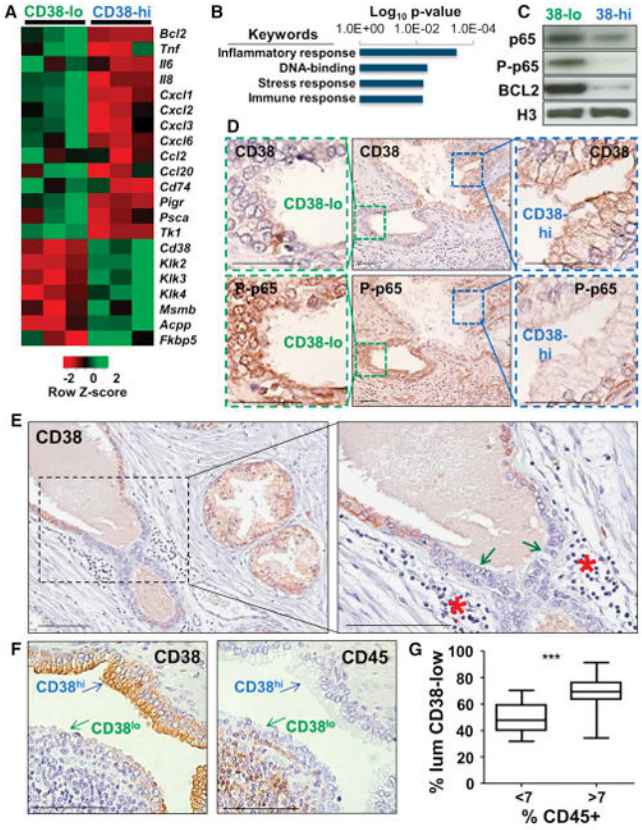

Figure 3. CD38^{lo} Luminal Cells Are Associated with Inflammation

(A) Heatmap of RNA-sequencing results of CD38^{lo} luminal cells and CD38^{hi} luminal cells from three independent patients.

(B) DAVID bioinformatics analysis (SP_PIR_ KEYWORDS) of the CD38^{lo} luminal gene signature with log(10) p values plotted.

(C) Western blot analysis of CD38^{lo} and CD38^{hi} luminal cells from a representative benign human prostate sample stained for total p65, phosphorylated p65 (P-p65 S536), BCL2, and histone H3 as a loading control.

(D) Immunohistochemical analysis of benign human prostate stained for CD38 and phosphorylated p65 (S536) on serial sections indicating an inverse relationship between expression of CD38 and P-p65. Scale bars, 50 μm.

(E) Immunohistochemical analysis of benign human prostate glands stained with anti-CD38 antibodies. Boxed regions are magnified in the bottom row. Arrows denote regions of epithelium with low expression of CD38 in close proximity to red asterisk identifying areas with immune cell infiltration. Scale bars, 100 μm.

(F) Immunohistochemistry on serial slides stained for CD38 and CD45. Scale bars, 100 μm.

(G) Increased proportion of luminal cells with CD38^{lo} phenotype from 29 samples plotted as CD45^{+} cells less than or greater than 7% of total prostate. Statistics represent two-tailed t test; ***p = 0.0003.

Author Manuscript Author Manuscript Author Manuscript Author Manuscript

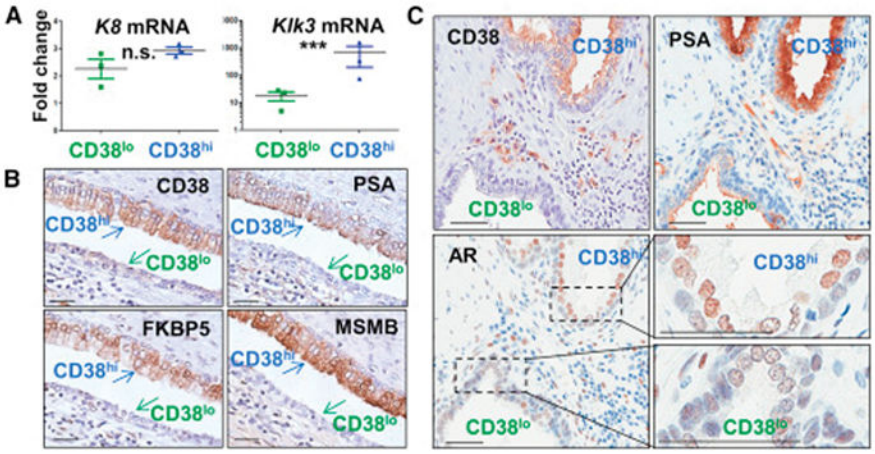

Figure 4. CD38^{lo} Luminal Cells Exhibit Reduced Androgen Signaling

(A) Relative expression of *Klk3* or *K8* compared to *Gapdh* in basal cells as measured by qPCR of basal, CD38^{lo}, and CD38^{hi} luminal cells isolated from three independent patient samples. Data are presented as mean ± SEM with replicate points shown. *Klk3* is shown on a log scale. Two-tailed unpaired t test between CD38^{lo} and CD38^{hi} luminal subsets; ***p = 0.0004.

(B) Immunohistochemical analysis of benign human prostate stained for CD38 and AR targets PSA, FKBP5, and MSMB. Scale bars, 100 μm.

(C) Immunohistochemistry for CD38, PSA, and AR distinguishes CD38^{hi} and CD38^{lo} regions. AR expression is magnified to demonstrate reduced expression in CD38^{lo} cells. Scale bars, 50 μm.

Author Manuscript Author Manuscript Author Manuscript Author Manuscript

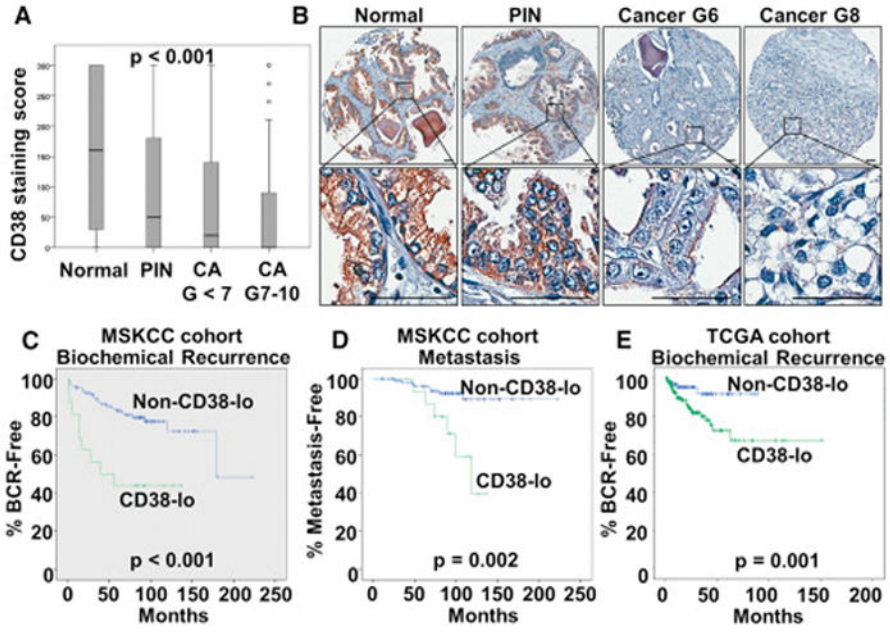

Figure 5. Association of CD38^{lo} Phenotype with Prostate Cancer Progression

(A) Plot of composite CD38 staining score in tissues histologically classified as normal, prostate intra-epithelial neoplasia (PIN), or prostate cancer (CA) with Gleason scores less than 7 or 7–10. Middle bar represents mean value. The overall effect of different levels of CD38 among the prostate regions was confirmed ($p < 0.001$).

(B) Representative immunohistochemical images of normal, PIN, Gleason 6, and Gleason 8 cancer stained for CD38, with high-power images below. Scale bars, 50 μm.

(C and D) Survival analysis from MSKCC cohort measuring biochemical recurrence (C) and metastasis (D) for tumors containing CD38 mRNA 1 SD below the mean compared to the remainder (non-CD38^{lo}). Log rank (Mantel Cox) $p < 0.001$ (recurrence in C) and $p = 0.002$ (metastasis in D).

(E) Survival analysis from the TCGA cohort measuring biochemical recurrence comparing CD38 expression less than (CD38^{lo}) or greater than (non- CD38^{lo}) the mean Z score. Log rank (Mantel Cox) $p = 0.001$.

Author Manuscript Author Manuscript Author Manuscript Author Manuscript

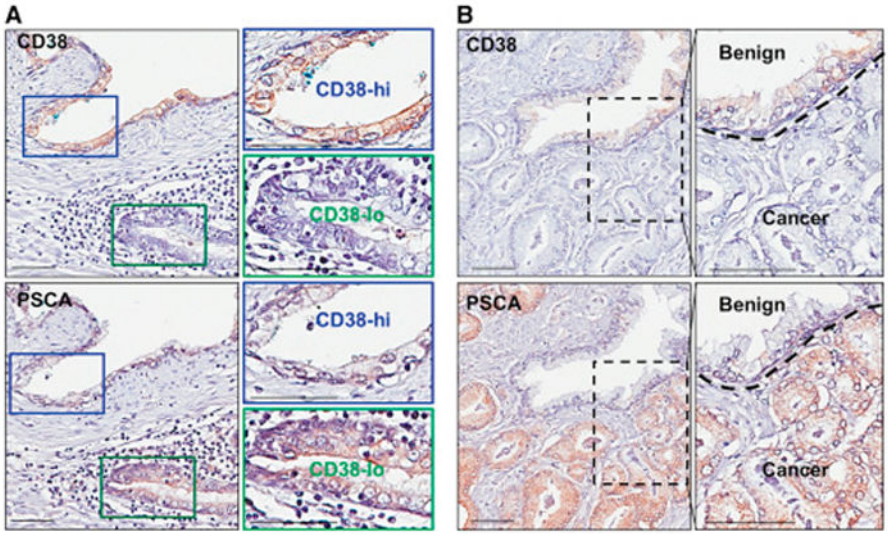

Figure 6. PSCA Is Expressed in CD38^{lo} Luminal Cells

(A) Serial sections of benign human prostate stained for CD38 and PSCA with boxed regions to magnify distinct CD38^{hi} PSCA-lo glands and inflammation-associated CD38^{lo} PSCA-hi cells.

(B) Serial sections of human prostate tissue stained for CD38 and PSCA with boxed region magnifying CD38^{hi} PSCA-lo benign tissue separated by a dotted line from CD38^{lo} PSCA-hi cancer. Scale bars, 50 μm.

Author Manuscript Author Manuscript Author Manuscript Author Manuscript

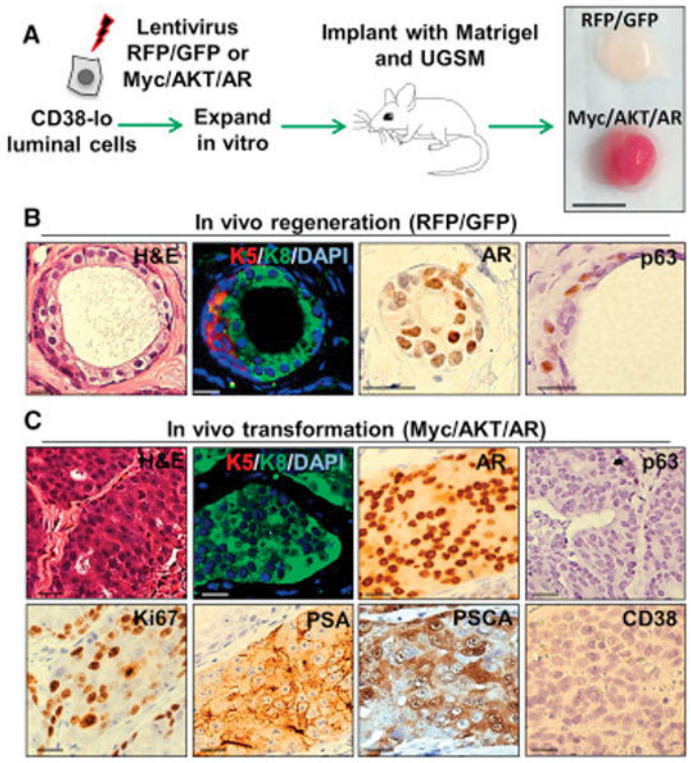

Figure 7. CD38^{lo} Luminal Cells Can Generate Glands and Initiate Human Prostate Cancer In Vivo

(A) Schematic representing experimental flow where CD38^{lo} luminal cells are transduced with lentivirus, expanded in vitro 7–10 days, combined with UGSM and Matrigel and implanted in vivo. Regenerated tissues from representative experiments are shown on the right. Scale bars, 5 mm.

(B) Representative in vivo regeneration of CD38^{lo} luminal cell-derived organoids transduced with control fluorescent GFP and red fluorescent protein (RFP) stained for H&E, K5, K8, DAPI nuclear counterstain, AR, and p63. Scale bars, 50 μm.

(C) Representative adenocarcinoma in regenerated tumor tissues from CD38^{lo} luminal cells transduced with Myc, AKT, and AR stained for H&E, K5, K8, DAPI nuclear counterstain, AR, p63, Ki67, PSA, PSCA, and CD38. Scale bars, 25 μm.